Figure 3 shows the dependence of average cloud diameter measured from the three exposures in each shot on the ejection delay time. The $B^{-1/2}$ curve is calculated from the known time dependence of the magnetic field. As can be seen from Fig. 3 the cloud has a diameter of less than 1 cm at peak compression. The initial diameter of the cloud, which is fixed by the injector location, is about 9 cm. The $B^{-1/2}$ curve is normalized in order to get the best fit for the experimental points. If the cloud behaves in an adiabatic way then one would expect a $B^{-1/2}$ dependence. But as can be seen from Fig. 3 the expansion of the cloud in the decaying magnetic field is faster.

The expansion of the cloud beyond the $B^{-1/2}$ dependence and the filling in of the center are both nonadiabatic processes and they are connected to the fact that the plasma is not neutral. As was shown earlier,[11] the cloud executes electrostatic oscillations which are similar in their nature to the diocotron oscillations.[10] These oscillations were always observed when the cloud was not neutralized and were never observed for neutralized clouds. As we described earlier the diocotron oscillations are surface modes which will tend to diffuse the surfaces of the cloud. It seems very reasonable, therefore, that the filling in of the center and the faster-than-adiabatic radial expansion are a result of these electrostatic oscillations. Filling in of the center is not occurring when the cloud is neutralized since these electrostatic modes do not exist for a neutralized cloud. This set of measurements represents an indirect evidence that one mechanism for a cross-field diffusion process in a nonneutral plasma is through the electrostatic oscillations of the plasma.

This work was supported by the National Science Foundation.

[1]C. A. Kapetanakos, R. E. Pechacek, D. M. Spero, and A. W. Trivelpiece, Phys. Fluids 19, 1555 (1971).
[2]V. P. Sarentsev, IEEE Trans. Nucl. Sci. 16, 15 (1969).
[3]D. Keefe, G. R. Lamberton, L. J. Laslet, W. A. Perkins, J. M. Peterson, A. M. Sessler, R. W. Allison, Jr., W. W. Chup, A. W. Luccio, and J. B. Rechen, Phys. Rev. Lett. 22, 558 (1969).
[4]C. Adelfinger *et al.*, in *Proceedings of the Ninth International Conference on High Energy Accelerators, Stanford, California, 1974* (National Technical Information Service, Springfield, Va., 1974), p. 218.
[5]R. E. Berg, H. Kim, M. P. Reiser, and G. T. Zorn, Phys. Rev. Lett. 22, 419 (1969).
[6]J. D. Daugherty, J. E. Eninger, and G. S. Janes, Phys. Fluids 12, 2677 (1968).
[7]W. Clark, P. Korn, A. Mondelli, and N. Rostoker, Phys. Rev. Lett. 37, 592 (1976).
[8]A. Irani and N. Rostoker, Part. Accel. 8, 107 (1978).
[9]S. Eckhouse, A. Fisher, R. Prohaska, and N. Rostoker, in Proceedings of the Third International Conference on Collective Ion Acceleration, Laguna Beach, California, 1978 (to be published).
[10]R. H. Levy, Phys. Fluids 8, 1288 (1965).
[11]S. Eckhouse, A. Fisher, and N. Rostoker, Phys. Fluids 21, 1840 (1978).

Hydrogen-Pellet Fueling Experiments on the ISX-*A* Tokamak

S. L. Milora, C. A. Foster, and P. H. Edmonds
Oak Ridge National Laboratory, Oak Ridge, Tennessee 37830

and

G. L. Schmidt
Plasma Physics Laboratory, Princeton University, Princeton, New Jersey 08540

We report the results of experiments on the ISX-*A* (impurity-study experiment) tokamak that demonstrate the technique of plasma fueling by solid-hydrogen-pellet injection. The results show that density increases of up to 30% or more can be realized without apparent deleterious effects on plasma stability and confinement.

Considerable attention has been given lately to the concept of proposed refueling tokamak fusion power reactors by injecting solid hydrogen pellets into the reacting plasma. The principal advantage claimed for this technique is that a moving pellet will traverse the confining magnetic fields and thereby carry fresh fuel to the hot central plasma core. For this technique to prove

successful, it is generally agreed that pellets must penetrate a significant fraction of the distance to the plasma axis before being consumed by the intense plasma heat. This requirement obviously favors large pellets, but heretofore, tokamak reactor design studies have not addressed the question of maximum pellet size and concomitant effects on plasma stability and transport.

In the first demonstration of this concept, small hydrogen pellets containing less than 1% of the total plasma-particle content were injected into the Oak Ridge Tokamak (ORMAK) at speeds of 1×10^4 cm/sec.[1] Because of their small size, these pellets penetrated a maximum distance of only 6 cm into the 25-cm plasma column and no detectable increase in plasma density was observed. In a somewhat different experiment,[2] large pellets were dropped through the axis of the pulsator device prior to initiation of the plasma discharge, resulting in attainment of substantially higher plasma densities than those achieved with standard hydrogen-gas prefill techniques. Although it may contribute to higher ultimate densities, this approach is not applicable to refueling during the course of the plasma discharge. In this paper, we report the results of recent experiments on the impurity-study experiment (ISX-*A*) tokamak in which large pellets containing 30 times more mass than used in ORMAK were injected into the existing plasma discharge at speeds exceeding 3×10^4 cm/sec. This resulted in a large observable fueling effect and deep penetration into the hot, high-density region of the plasma.

The experiment is illustrated schematically in Fig. 1. The pellet injector is a gun-type design[3] that accelerates nominally cylindrical pellets of ~0.6 mm in diameter and 0.6–0.85 mm in length to average speeds of 3.3×10^4 cm/sec. Some irregularity in size is inherent, but pellets typically contain $(0.6–1.4)\times10^{19}$ hydrogen atoms. Pellets are detected by a photodiode at the gun-barrel exit plane and enter the tokamak chamber through a 3.8-cm-diam aperture. A second photodiode located in the pellet drift tube views the pellet-plasma interaction from behind and records the light emanating from the luminous cloud of neutral hydrogen that surrounds the pellet. The pellet ablation rate is inferred from this measurement,[1] and the time interval between responses of the photodiode pair determines the pellet velocity.

The ISX-*A* device has a minor radius of 26 cm and a major radius of 92 cm (plasma volume $=1.23\times10^6$ cm^3). The plasma was Ohmically heated at 120 kA, giving a safety factor of 3.3 at the plasma edge with a toroidal magnetic field of 13.2 kG. Standard tokamak diagnostics are employed including microwave interferometry for line-averaged electron density measurements, laser-Thomson scattering for radial electron temperature and density profiles, and magnetic probe measurements to monitor the level of magnetohydrodynamic activity (Mirnov oscillations). Pyroelectric detectors (radiometer) monitor the total power incident on the vacuum liner from radiation and charge-exchange losses from the plasma. Photographs taken from a window located above the pellet injection port provide a determination of the pellet trajectory in the plasma.

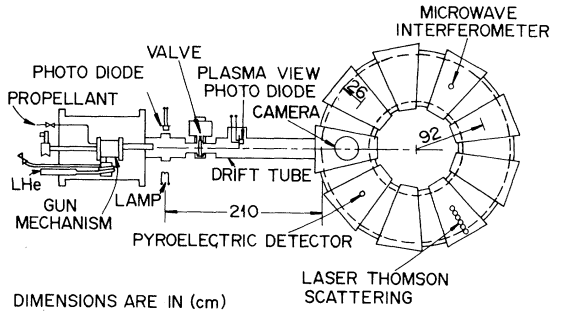

FIG. 1. Schematic of experimental arrangement showing pellet injector, tokamak, and the location of relevant plasma diagnostics. A single H_2 pellet is formed within the liquid-helium–cooled gun mechanism and expelled during the tokamak discharge by helium-gas propellant. A fast gate valve opens to allow the pellet to enter the drift tube.

The rate at which neutral hydrogen particles are emitted at the pellet surface (ablation rate) is balanced by ionizations occurring within the cloud surrounding the pellet. For electron impact ionizations, the ratio of the rate of production of H_α photons to the ionization rate of neutrals is roughly a constant over the range of electron temperatures encountered by the pellet. To a first approximation the ablation rate is therefore proportional to the H_α signal. The proportionality constant is evaluated *a posteriori* as the ratio of the total number of injected ions, ΔN, to the integrated light signal, $\int s\,dt$. Accordingly, the ablation rate is given by

$$dN/dt = \text{ablation rate} = Ks = (\Delta N)s/\int s\,dt. \quad (1)$$

Typical pellet ablation records determined using

this relationship are presented as a function of penetration depth into the plasma in Fig. 2. Two distinctly different ablation modes are observed which we designate as type A (predominant) and type B. The form of the type-A ablation is qualitatively similar to that observed in the ORMAK experiments—a gently rising region followed by a rapid increase and abrupt decrease to extinction. The penetration depth, as inferred from the pellet velocity and the time duration of the light emission from the pellet (~350 μsec), is in good agreement with the values (12.4±1.2 cm) determined photographically.

The photographs also reveal that the visible-light emission from the neutral cloud is predominantly H_α radiation (300 W typical) and that the cloud attains a maximum width of ~5 cm. As was the case in ORMAK, the pellets were observed to deviate from their initial radial trajectory, curving slightly in the direction of the electron drift velocity.

In Fig. 2, both ablation types are compared with a modified version[4] of the neutral-gas shielding models of Parks, Turnbull, and Foster,[5] and Vaslow.[6] The calculation assumes an equivalent spherical pellet size of 0.64 mm, which was inferred from the magnitude of the plasma density rise following injection (as measured by the microwave interferometer). The type-B ablation, which occurred less frequently (~25% of the time), cannot be explained satisfactorily by the model, given the temperature and density profiles characteristic of the ISX device. The high initial ablation rate is indicative of a steeply rising electron temperature profile in the plasma edge. However, it cannot be concluded that plasma conditions alone are responsible for the occurrence of the type-B ablation until more complete measurements of the edge plasma parameters are made and additional information concerning the nature of individual pellets (such as exact size and shape, structural integrity, and consistency) is available.

The effect of pellet injection on the line-averaged electron density as measured by the microwave interferometer is shown in Fig. 3 for the examples of Fig. 2. A sharp initial rise in signal is observed at the interferometer station ~100 μsec following pellet injection, indicating a toroidal transport velocity of 2×10^6 cm/sec. The signal rise time of ~300 μsec is comparable

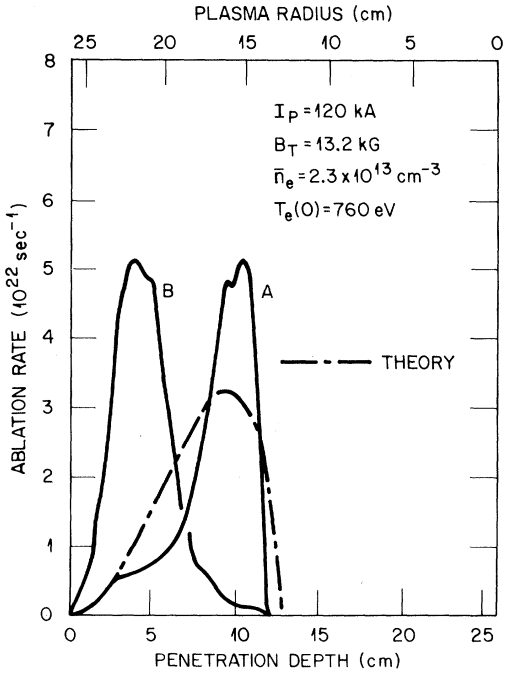

FIG. 2. Pellet ablation rates as a function of position in plasma for type-A and type-B modes. Pellet velocity is 3.5×10^4 cm/sec; diameter, 0.64 mm; $\Delta N = 6\times10^{18}$. The theoretical calculation assumes that T_e and n_e vary as $T_e = T_e(0)[1-(r/a)^2]^2$ and $n_e = \frac{3}{2}\bar{n}_e[1-(r/a)^2]$, where r is the plasma radius. The assumed profiles are in agreement with laser–Thomson-scattering measurements.

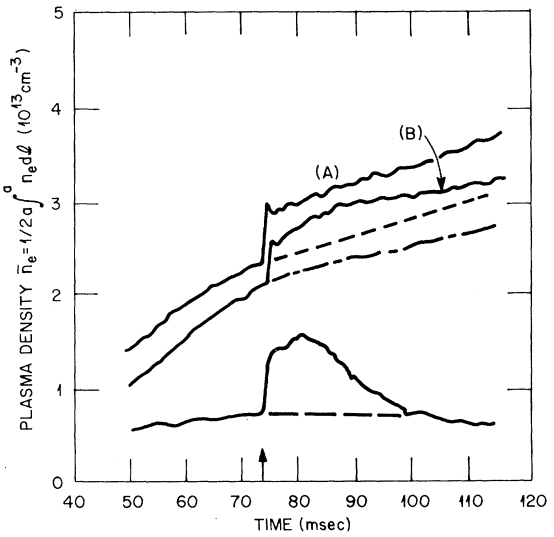

FIG. 3. Line-averaged electron density as measured by microwave interferometer for the examples of Fig. 2. Dashed lines represent plasma behavior without injection. Density variations are produced by differing gas puffing rates.

to the observed pellet lifetime, and the magnitude of the density rise corresponds to the ion content of an equivalent spherical pellet of 0.64 mm in diameter (containing 6×10^{18} hydrogen atoms).

The distinction between the two ablation types is characterized by the density behavior subsequent to this initial $\Delta\bar{n}_e$. For type-*A* ablation, the density remains elevated above the normal device density behavior by exactly this amount for the duration of the discharge. The density trace for type-*B* ablation exhibits a noticeable additional buildup that takes place within a 20-msec time interval. Part of this behavior is likely due to the chordal (as compared to volumetric) averaging of the microwave interferometer and diffusion of fuel into the interior of the plasma. Fuel which is initially deposited over the outer magnetic flux surfaces will diffuse inward, eventually carrying a larger fraction of the added plasma into view of the interferometer. Such an effect would be less pronounced for fuel which is initially deposited more deeply in the plasma, such as in type-*A* ablation. The observed buildup might also be a result of hydrogen desorption from the walls of the device and of particle recycling effects at the plasma limiter. These effects would be more pronounced for type-*B* ablation because of the greater outward diffusion of plasma. The fact that the density remains elevated for the duration of the discharge in both instances is evidence that the addition of relatively large amounts of cold fuel ($\Delta\bar{n}_e/\bar{n}_e \cong 0.3$) does not adversely affect plasma stability or confinement.

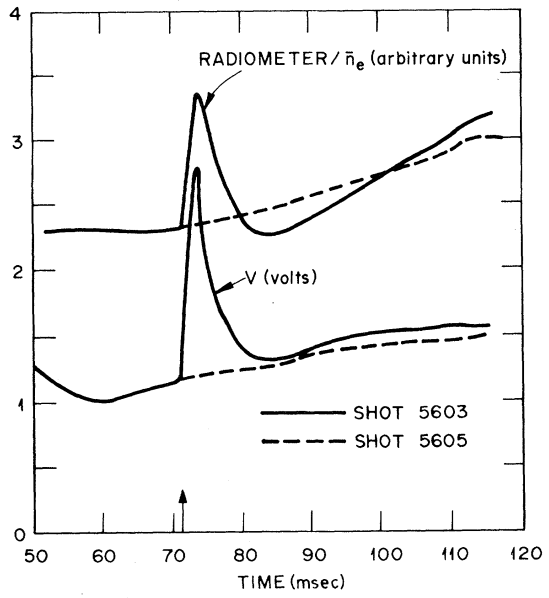

FIG. 4. Plasma electromotive force and normalized radiometer signals as a function of time showing effect of pellet injection. Dashed lines represent plasma behavior without injection.

Pellets were injected into a low-density equilibrium plasma to determine the effect on the plasma discharge of massive addition of cold material ($\Delta\bar{n}_e/\bar{n}_e \gtrsim 1$). As illustrated by the low-density example of Fig. 3, the density remains elevated briefly after injection and is followed by a gradual decay to the equilibrium level in a time interval of 20 msec. Large-scale Mirnov oscillations ($m = 2$) were observed in conjunction with the onset of the density decay, but their amplitude returned to normal levels upon density equilibration. Large localized cooling effects resulting from introduction of the pellet are possibly responsible for the enhanced transport, although the observed density decay might also be a consequence of the sudden elevation of the plasma density far above the equilibrium state.

An indication of the extent of plasma cooling subsequent to pellet injection is given in Fig. 4, where the plasma voltage and normalized radiometer signal are presented. Both signals increase abruptly at the instant of injection, which is consistent with a significant cooling effect. With no discernible change in plasma current, the loop voltage increase is attributable to increased resistivity. The cooling of impurities (mostly oxygen) in the outer regions of the discharge normally results in enhanced line radiation, and the radiometer increase indicates this. Both signals decay to normal levels (i.e., without injection) in a time interval of 13 msec. These effects have been observed in particle transport calculations that simulate pellet injection.[7]

The voltage data indicate that the incremental Ohmic-heating energy associated with pellet injection is proportional to the observed increment in plasma density. An average of 475 ± 80 eV is expended for each charged particle that is added before equilibrium is reestablished. Single bursts of hydrogen gas injected into the plasma give qualitatively similar results with the exception that the Ohmic power input is larger (600–700 eV/particle) and the power lost to the wall by radiation is larger by a factor of 2. These observations are in agreement with the line of reasoning that plasma added to the edge will exhibit higher losses due to increased diffusive

and impurity radiation effects than fuel added more deeply as with pellet injection. It also demonstrates that pellet fueling is more efficient than gas puffing.

We have demonstrated that relatively large pellets can be injected into a tokamak plasma, resulting in substantial increases in density. The advantages which may arise from this technique are twofold: (1) The technological difficulties associated with fueling by injection of pellets at high velocity may be eased because for a given penetration depth, large pellets require lower velocities than do smaller pellets, and (2) fueling by deep pellet injection appears to be more efficient from the point of view of plasma heating requirements than does edge fueling by gas injection.

The authors wish to acknowledge the assistance of the Tokamak Experimental Section and in particular C. E. Bush, J. L. Dunlap, R. C. Isler, P. W. King, D. H. McNeill, J. T. Mihalczo, and J. B. Wilgen. The discussions with and contributions of H. C. Howe and M. Murakami are also gratefully acknowledged. This research was sponsored by the Office of Fusion Energy (ETM), U. S. Department of Energy under Contract No. W-7405-eng-26 with the Union Carbide Corporation.

[1]C. A. Foster, R. J. Colchin, S. L. Milora, K. Kim, and R. J. Turnbull, Nucl. Fusion 17, 1967 (1977).

[2]W. Amenda, K. Büchl, R. Lang, L. L. Lengyel, and W. Riedmüller, in Proceedings of the Fusion Fueling Workshop, Princeton, New Jersey, 1977, CONF-771129 (unpublished).

[3]S. L. Milora and C. A. Foster, ORNL Report No. ORNL-TM-6598 (to be published).

[4]S. L. Milora and C. A. Foster, "A Revised Neutral Gas Shielding Model for Pellet-Plasma Interactions" (to be published).

[5]P. B. Parks, R. J. Turnbull, and C. A. Foster, Nucl. Fusion 17, 539 (1977).

[6]D. F. Vaslow, IEEE Trans. Plasma Sci. 5, 12 (1977).

[7]H. C. Howe, private communication.

Evidence for a New Phase Transition in Solid ^{3}He in High Magnetic Fields

E. A. Schuberth,[a] D. M. Bakalyar, and E. D. Adams
Physics Department, University of Florida, Gainesville, Florida 32611

(Received 24 August 1978)

Liquid and solid ^{3}He have been cooled by adiabatic compression to the solid ordering temperature in fields of 2.0 and 2.8 T. Chart traces of pressure versus time show a new feature which suggests a first-order transition near the A_1-A_2 superfluid transitions.

Exchange interactions in solid ^{3}He are sufficiently strong to produce a magnetic transition of the nuclear spins to an ordered state at a much higher temperature than for classical dipoles. In several recent studies,[1-3] this phase transition has been observed near 1 mK. In low magnetic fields, the transition is antiferromagnetic and may possibly be first order.[3,4] In magnetic fields greater than 0.42 T, the melting pressure data of Kummer, Mueller, and Adams[2] (KMA) show that the ordering is of a different type. Thermodynamic analysis[4] of the KMA data suggests a second-order transition to a weakly ferromagnetic or pseudoferromagnetic state. In the present work, the transition has been studied in magnetic fields of 2.0 and 2.8 T. The most striking result is the appearance of a new feature which suggests a phase transition in the solid near the A_1 and A_2 superfluid transitions.

A mixture of liquid and solid ^{3}He was cooled along the melting curve to a minimum of 0.85 mK (in low fields) using the Pomeranchuk compression cell described by KMA. The experiment consisted of qualitative observations of ^{3}He pressure P_3 versus time during the compressions, and of preliminary measurements of the latent heat of melting, from which the melting pressure and entropy versus temperature were obtained.

The new phase transition displays itself dramatically in the chart traces of P_3 versus time shown in Fig. 1. The first curve is for $B = 2.0$ T and all the others are for $B = 2.8$ T but at different compression rates. Following the changes in slope at the A_1 and A_2 superfluid transitions[5] (indicated by arrows), a new feature appears as an abrupt backstep in pressure, which we believe indicates a new phase transition in solid ^{3}He, as will be discussed below. (This backstep is similar to that seen at the superfluid B transition, suppressed for $B > 0.5$ T.) On a given compression

